

Synthesis and Properties of CaFe_2As_2 Single Crystals

F. Ronning¹, T. Klimczuk^{1,2}, E.D. Bauer¹, H. Volz¹, J.D. Thompson¹

¹*Los Alamos National Laboratory, Los Alamos, New Mexico 87545, USA*

²*Faculty of Applied Physics and Mathematics,*

Gdansk University of Technology, Narutowicza 11/12, 80-952 Gdansk, Poland

(Dated: October 22, 2018)

Abstract

We report the synthesis and basic physical properties of single crystals of CaFe_2As_2 , an isostructural compound to BaFe_2As_2 which has been recently doped to produce superconductivity. CaFe_2As_2 crystalizes in the ThCr_2Si_2 structure with lattice parameters $a = 3.887(4)$ Å and $c = 11.758(23)$ Å. Magnetic susceptibility, resistivity, and heat capacity all show a first order phase transition at $T_0 = 171$ K. The magnetic susceptibility is nearly isotropic from 2 K to 350 K. The heat capacity data gives a Sommerfeld coefficient of 8.2 ± 0.3 mJ/molK², and does not reveal any evidence for the presence of high frequency (> 300 K) optical phonon modes. The Hall coefficient is negative below the transition indicating dominant n-type carriers.

PACS numbers:

The discovery of superconductivity in the oxypnictide compounds $\text{RFeAs}(\text{O}_{1-x}\text{F}_x)$ ($\text{R} = \text{La, Ce, Pr, Nd, Sm, Gd}$) with the ZrCuSiAs structure type has stimulated a wealth of activity around the globe [1, 2, 3, 4, 5, 6, 7]. The similarity of this system and the cuprates with respect to the layered structure and the phase diagram with carrier doping, suggests that the physics may be similar. The fact that the parent compounds are metallic indicates additional similarity to the heavy fermion superconductors [8, 9, 10].

If the FeAs layers are critical for the relatively high superconducting transition temperatures then it does not come as a big surprise that superconductivity was found in the related ThCr_2Si_2 structure. Hole-doping by potassium in BaFe_2As_2 and SrFe_2As_2 produces superconductivity up to $T_c = 38 \text{ K}$. [13, 18, 19]. Given the relatively high transition temperatures and that single crystals appear relatively easier to synthesize than those in the RFeAsO family, the ThCr_2Si_2 structure may be a more ideal system for elucidating the physics of these new Fe-based superconductors. Currently, the AFe_2As_2 compounds are known to be stable with divalent $\text{A} = \text{Ba, Sr, and Eu}$ [11, 20], of which only the $\text{A} = \text{Ba}$ and Sr compounds so far have been doped to produce superconductivity [13, 18, 19]. In this paper we report on the synthesis and basic physical properties of single crystals of CaFe_2As_2 . A sharp first order anomaly is observed by susceptibility, heat capacity and electrical transport measurements at $T_0 = 171 \text{ K}$.

Single crystals of CaFe_2As_2 were grown in Sn flux in the ratio $\text{Ca:Fe:As:Sn}=1:2:2:20$. The starting elements were placed in an alumina crucible and sealed under vacuum in a quartz ampoule. The ampoule was placed in a furnace and heated to $500 \text{ }^\circ\text{C}$ at $100 \text{ }^\circ\text{C hr}^{-1}$, and held at that temperature for 6 hours. This sequence was repeated at $750 \text{ }^\circ\text{C}$, $950 \text{ }^\circ\text{C}$ and at a maximum temperature of $1100 \text{ }^\circ\text{C}$, with hold times of 8 hr., 12 hr., and 4 hr, respectively. The sample was then cooled slowly ($\sim 4^\circ\text{C hr}^{-1}$) to $600 \text{ }^\circ\text{C}$, at which point the excess Sn flux was removed with the aid of a centrifuge. The resulting plate-like crystals of typical dimensions $5 \times 5 \times 0.1 \text{ mm}^3$ are micaceous and ductile and are oriented with the c -axis normal to the plate. CaFe_2As_2 crystallizes in the ThCr_2Si_2 tetragonal structure (space group no. 139) (Fig. 1) with lattice parameters $a = 3.887(4) \text{ \AA}$ and $c = 11.758(23) \text{ \AA}$ as revealed by the powder x-ray diffraction pattern shown in Fig. 2. In this structure, layers of Ca are capped by Fe-As tetrahedra along the c -axis. These Fe-As tetrahedra are the common structural units to the Fe-based RFeAsO and AFe_2As_2 superconductors.

Magnetic measurements were performed from 1.8 K to 300 K using a commercial SQUID

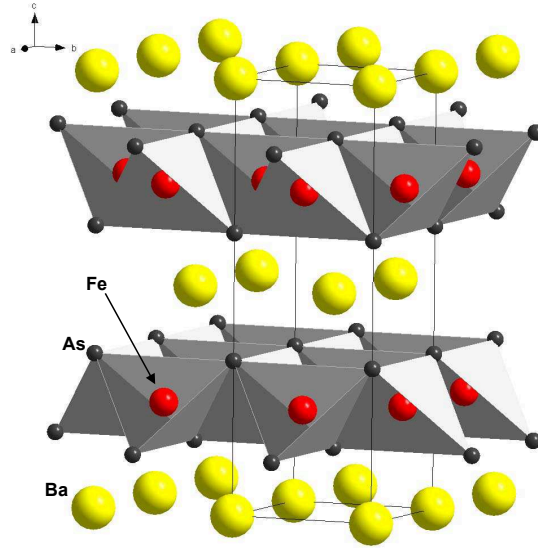


FIG. 1: Crystal structure of CaFe_2As_2

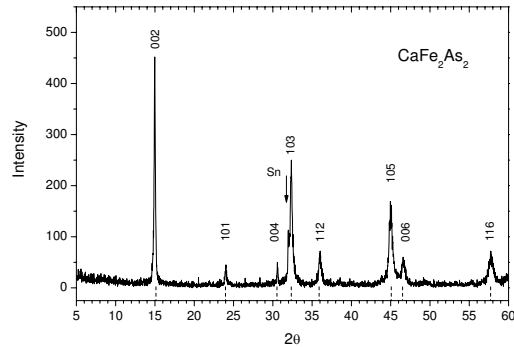


FIG. 2: Powder X-ray diffraction pattern ($\text{CuK}\alpha$ radiation) for CaFe_2As_2 . Vertical bars at the bottom represent the Bragg peak positions for the ThCr_2Si_2 tetragonal ($I4/mmm$) structure with refined cell parameters $a = 3.887(4) \text{ \AA}$ and $c = 11.758(23) \text{ \AA}$. Miller indices for each peak are shown, and a peak from the Sn flux is marked with an arrow.

magnetometer. Specific heat measurements were carried out using an adiabatic method in a commercial cryostat from 2 K to 300 K. Electrical transport measurements were performed using a LR-700 resistance bridge with an excitation current of 1 mA, on samples for which platinum leads were spot welded.

The magnetic susceptibility $\chi(T)$ of CaFe_2As_2 measured in a magnetic field $H = 5$ T with $H||ab$ and $H||c$ is shown in Fig. 3. The susceptibility is essentially isotropic over the entire measured temperature range. Close to $T_0 = 172$ K a sharp drop is evident in χ_{ab} and in χ_c , albeit slightly smaller, likely indicating a structural transition that is similar to those observed in BaFe_2As_2 [12, 14, 18] and LaFeAsO [1].

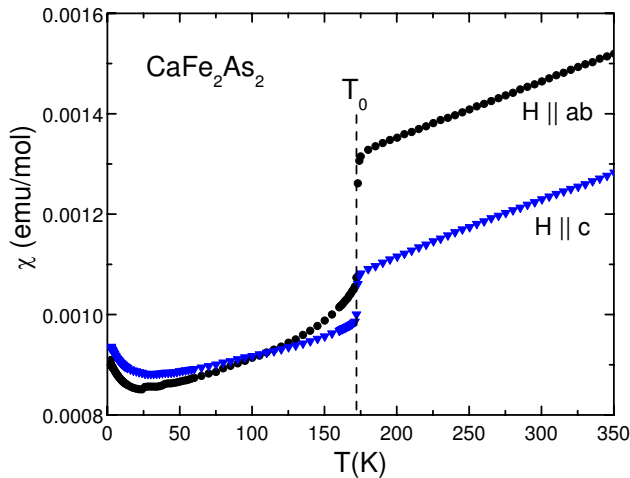


FIG. 3: Magnetic susceptibility $\chi(T)$ of CaFe_2As_2 measured in a magnetic field $H = 5$ T for $H||ab$ (black circles) and $H||c$ (blue triangles). A structural transition is indicated by the sharp drop at $T_0 = 172$ K (dashed line) in χ_c and χ_{ab} .

The heat capacity presented in figure 4 reveals a very sharp symmetric anomaly consistent with a first order phase transition at 172 K (upon warming). In the top inset, the relaxation curve of sample temperature versus time is shown. While a constant heat is applied to the sample it steadily increases in temperature as dictated by the sample heat capacity and the thermal link to the bath. The plateau in the curve indicates an abrupt increase in the heat capacity as well as the latent heat associated with the first order transition[23], sharply defined in temperature at 171.8 ± 0.1 K. The low temperature heat capacity is presented in the lower inset. Below 10 K the heat capacity data can be fit to $C = \gamma T + \beta T^3 + \alpha T^5$. This gives an electronic specific heat coefficient of $\gamma = 8.2 \pm 0.3$ mJ/mol K². Assuming that the

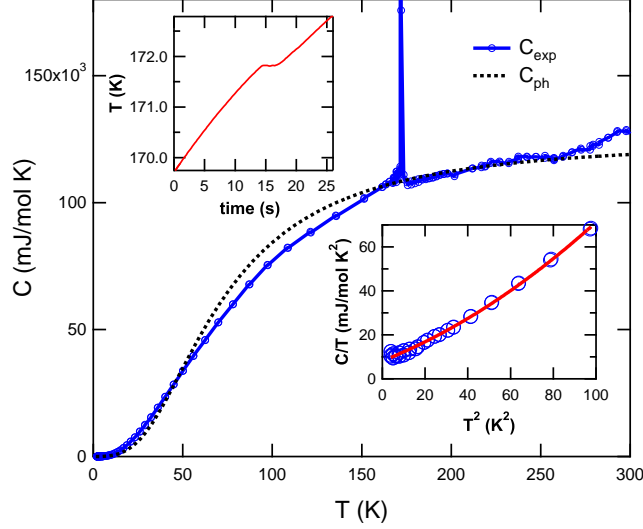


FIG. 4: Specific heat versus temperature is shown for CaFe_2As_2 . The dashed line represents a simple lattice estimate as described in the text. The top inset displays the relaxation curve at the transition temperature. The lower inset displays the low temperature heat capacity. The solid line is a fit to $C/T = \gamma + \beta T^2 + \alpha T^4$.

T^3 term is entirely due to acoustic phonons, from the β coefficient = 0.383 ± 0.018 mJ/mol K^4 we extract a Debye temperature $\Theta_D = 292$ K. The dashed curve in the figure gives the lattice contribution to the specific heat based upon a simple Debye model using $\Theta_D = 292$ K. While this is certainly an oversimplification of the exact phonon density of states, the fact that this gives a reasonable account of the data at high temperatures indicates that there are relatively few high frequency optical phonon modes with energies above 300 K. This is in contrast to the case of phonon-mediated superconductor MgB_2 [24], where analysis of the heat capacity indicates the presence of phonon modes up to 750 K.

As with susceptibility and heat capacity, the resistivity data presented in figure 5 contains a clear first order phase transition at 170 K. The jump indicates either an increase in scattering or a decrease in the number of carriers below the transition relative to above it. The samples have a RRR ($= \rho(300 \text{ K})/\rho(4 \text{ K})$) of 10. A small partial superconducting transition at 3.8 K is due to small Sn inclusions. Data for current parallel to the c -axis on 4 samples (not shown) have a qualitatively similar temperature dependence, but range in absolute magnitude from 50 to 1000 times larger than the in-plane data, possibly a consequence of weakly coupled micaceous layers leading to large variations in the magnitude

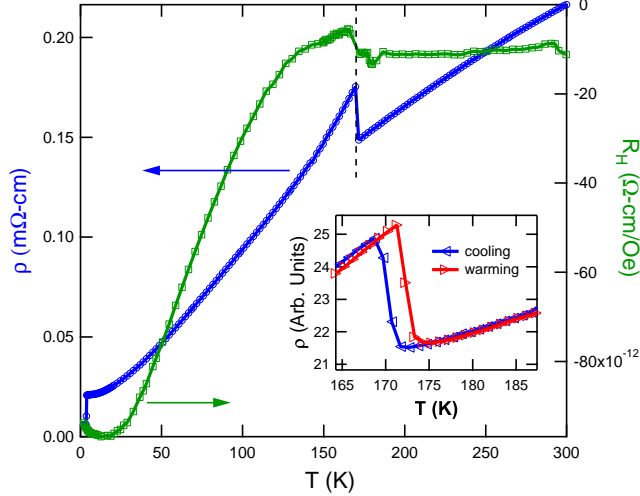


FIG. 5: In-plane resistivity ($\rho_{\parallel ab}$) and the Hall coefficient of CaFe_2As_2 as a function of temperature. The inset illustrates the thermal hysteresis at the transition observed in resistivity for current along the c -axis.

of the c -axis resistivity. The inset demonstrates the thermal hysteresis expected for a first order phase transition. Also shown in Fig. 5 is the Hall coefficient. The dominant carrier below the 171 K transition is electron-like. There is a role-over at 15 K which may be due to either the multiband nature of these systems, or due to localization effects. With a resolution of $2 \times 10^{-11} \text{ } \Omega\text{-cm/Oe}$ we can not say whether the dominant carrier type at room temperature is also electron-like.

TABLE I: Comparison of properties of known AFe_2As_2 compounds where A is a divalent atom.

Compound	a (\AA)	c (\AA)	Θ_D (K)	γ (mJ/molK^2)	T_0 (K)	refs.
CaFe_2As_2	3.887(4)	11.758(23)	292	8.2(3)	171	this work
EuFe_2As_2	3.911(1)	12.110(4)			195	[20, 21, 22]
SrFe_2As_2	3.927(6)	12.37(2)	196	3.3 ¹	200(5)	[11, 16, 17]
BaFe_2As_2	3.962(6)	13.04(2)	134,200	6,16,37	80-140	[11, 12, 14, 15]

¹ Ref [16] report $\gamma = 33 \text{ mJ/mol K}^2$, but the figure indicates a value between 11 and 3.3 mJ/mol K^2 .

Briefly, we compare our results with currently available data on other members of the AFe_2As_2 compounds with $A = \text{Ba, Sr, and Eu}$, listed in Table 1. We note that the lattice constants monotonically decrease from BaFe_2As_2 to SrFe_2As_2 to EuFe_2As_2 to CaFe_2As_2 , as

one would expect given the smaller ionic radii of Ca^{2+} versus Eu^{2+} and Sr^{2+} versus Ba^{2+} . The higher Debye temperature for CaFe_2As_2 (292 K) is consistent with the smaller unit cell volume. However, the structural/SDW phase transition is not monotonic with cell volume even within the group IIA of the periodic table ranging from 80-140 K for BaFe_2As_2 , and 195-205 K in SrFe_2As_2 compared with 170 K in CaFe_2As_2 . (EuFe_2As_2 orders at 195 K, and the Eu moments order at 20 K[21].) The reason for this is not understood, but possibly indicates the sensitivity of the transition to details of the electronic structure. Similarly, the anisotropy of the susceptibility of CaFe_2As_2 measured at 5 T is nearly isotropic over the entire temperature range measured, both above and below the transition. Although the overall magnitude is similar to that observed in SrFe_2As_2 [16] the anisotropy is qualitatively different. In our case the low temperature Curie-Weiss tail is isotropic, and thus could originate from an impurity contribution. The isotropic behavior above the transition is more consistent with that observed in BaFe_2As_2 [14]. The role of trace amounts of ferromagnetic impurity phases such as Fe_2As [25], will be studied in more detail to determine the intrinsic behavior of the susceptibility. Finally, whether the current samples are affected by Sn substitution as suggested for single crystals of BaFe_2As_2 grown by a similar technique [14] must still be investigated.

We have synthesized single crystals of CaFe_2As_2 , which possesses a first order transition at 170 K, which is likely a combined structural and magnetic transition. Given that superconductivity has been found by doping the isostructural Ba and Sr compounds[13, 18, 19] we believe that the Ca compound is also a likely candidate for the presence of superconductivity upon chemical substitution.

At the completion of this work we became aware of two other papers reporting the synthesis of CaFe_2As_2 . Single crystals of CaFe_2As_2 grown using self flux[26] and Sn flux[27] methods gave results similar to ours, and indeed superconductivity was found upon Na doping[26].

Acknowledgments

We acknowledge useful discussions with B. Scott. Work at Los Alamos National Laboratory was performed under the auspices of the U.S. Department of Energy.

- [1] Y. Kamihara, T. Watanabe, M. Hirano, H. Hosono, *J. Am. Chem. Soc.* **130**, 3296 (2008).
- [2] X.H. Chen, et. al., *Nature* **453**, 761 (2008).
- [3] Z.-A. Ren, et. al., *Chin. Phys. Lett.* **25**, 2215 (2008).
- [4] G.F. Chen, et. al., *Phys. Rev. Lett.* **100**, 247002 (2008).
- [5] Z.-A. Ren, et. al., *Europhys. Lett.* **82**, 57002 (2008).
- [6] Z.-A. Ren, et. al., arXiv:0803.4283 , (2008).
- [7] P. Cheng, et. al., *Science in China G* **51**, 719 (2008).
- [8] N.D. Mathur, et. al., *Nature* **394**, 39 (1998)
- [9] T. Park, et. al., *Nature* **440**, 65 (2006)
- [10] H.Q. Yuan, et. al., *Science* **302**, 2104 (2003)
- [11] M. Pfisterer, G. Nagorsen, *Z. Naturforsch. B: Chem. Sci.* **35**, 703 (1980).
- [12] M. Rotter, M. Tegel, D. Johrendt, I. Schellenberg, W. Hermes, R. Poettgen, arXiv:0805.4021 , (2008).
- [13] M. Rotter, M. Tegel, D. Johrendt, arXiv:0805.4630 , (2008).
- [14] N. Ni, et. al., arXiv:0806.1874 , (2008).
- [15] J.K. Dong, et. al., arXiv:0806.3573 , (2008).
- [16] J.-Q. Yan, et. al., arXiv:0806.2711 , (2008).
- [17] C. Krellner, et. al., arXiv:0806.1043 , (2008).
- [18] G.F. Chen, et. al., arXiv:0806.1209 , (2008).
- [19] K. Sasmal, et. al., arXiv:0806.1301 , (2008).
- [20] R. Marchand, W. Jeitschko, *J. Solid State Chem.* **24**, 351 (1978).
- [21] H. Raffius, et. al., *J. Phys. Chem. Solids.* **54**, 135 (1993).
- [22] H.S. Jeevan, Z. Hossain, C. Geibel, P. Gegenwart, arXiv:0806.2876 , (2008).
- [23] J. Lashley, et. al., *cryogenics* **43**, 369 (2003)
- [24] Ch. Wälti, et. al., *Phys. Rev. B* **64**, 172515 (2001)

- [25] I. Nowik, I. Felner, arXiv:0806.4078 , (2008).
- [26] G. Wu, et. al., arXiv:0806.4279 , (2008).
- [27] N. Ni, et. al., arXiv:0806.4328 , (2008).